Phase-Bifurcation Cosmogenesis: A Dynamical Framework for Synchronization, Antipodal Locking, and Non-Relaxation in CPT-Symmetric Twin Universes

Cosmic Thinker & ChatGPT (Toko)

November 13, 2025

Abstract

We study the dynamical evolution of the phase difference $\Delta\phi$ between two CPT-mirrored cosmological sectors, each evolving forward in its own arrow of time. The phase follows a damped, driven equation of motion in a periodic axion-like potential with cosmological Hubble friction and a decaying rotational source. Using large ensembles of numerical trajectories, we identify three late-time behaviours: synchrony (A, $\Delta\phi \to 0$), antipodal locking (B, $\Delta\phi \to \pi$), and non-relaxation/escape (C), the latter defined as failure to settle into any attractor within the finite integration window.

We map the A/B/C sectors across the parameter space $(m_\phi, k_{\rm rot}, \Delta\phi_{\rm ini})$, establishing that: (i) the boundaries are smooth (non-fractal), (ii) the fate probabilities are dominated by the effective phase mass m_ϕ, (iii) the rotational coupling $k_{\rm rot}$ influences only transient dynamics, (iv) the synchrony probability $P_A(m_\phi)$ has a clean monotonic transition with a well-defined critical value $m_{\phi,\rm crit} \simeq 1.965$, and (v) the two-dimensional probability landscape $P_A(m_\phi, k_{\rm rot})$ exhibits nearly vertical transition bands.

We discuss cosmological implications for coherence, possible relic asymmetries, EB/TB signatures, and the interpretation of phase-bifurcation as a mechanism for inter-sector synchronisation in CPT-symmetric cosmology. A full reproducibility package (code, data, CSV sector maps, and integration scripts) is provided separately in an open GitHub+Zenodo release.

1 Introduction

CPT-symmetric cosmologies [1] posit that the Big Bang produced two time-reversed sectors related by a global CPT transformation. In such scenarios, the relative phase $\Delta\phi$ between the sectors is a natural dynamical degree of freedom controlling interference, coherence, and possible physical asymmetries. Whether $\Delta\phi$ synchronises, drifts, or becomes trapped near unstable configurations is crucial for understanding the phenomenology of these models.

Early heuristic arguments suggested that the phase-fate diagram might exhibit fractal boundaries, akin to nonlinear driven oscillators. In this work we rigorously test this expectation using a physically motivated phase model with:

- a periodic axion-like potential,
- cosmological Hubble damping,
- a rotational source that decays with expansion,
- forward evolution in $N = \ln a$ across ~ 9.2 e-folds.

We demonstrate that:

- the A/B/C regions are smooth, non-fractal,
- m_ϕ almost entirely controls the phase fate,
- $k_{\rm rot}$ barely affects final outcomes,
- a clean critical mass $m_{\phi,\rm crit} \simeq 1.965$ exists,
- sector C corresponds to non-relaxation over cosmological time,

and we provide a full reproducibility package via GitHub and Zenodo.

Figure 1 gives a schematic overview.

Figure 1: Global schematic of the phase-bifurcation framework.

2 Theoretical framework

2.1 Periodic axion-like potential

We take:

$$V_{\text{eff}}(\Delta\phi) = V_0\big[1 - \cos(\Delta\phi)\big],$$

with minima at $0, 2\pi, \ldots$ and maxima at $\pi, 3\pi, \ldots$. Near any minimum the quadratic approximation holds:

$$V_{\text{eff}} \simeq \frac{1}{2} m_\phi^2 \Delta\phi^2.$$

2.2 Rotational coupling and cosmological damping

We model misalignment through:

$$J_{\text{rot}}(t) = k_{\text{rot}}\, a^{-\gamma}(t), \qquad \gamma = 2.$$

The Lagrangian is:

$$\mathcal{L} = \frac{1}{2} a^3 (\dot{\Delta\phi}^2 - m_\phi^2 \Delta\phi^2) + a^3 J_{\text{rot}} \Delta\phi.$$

The cosmic-time EOM is:

$$\ddot{\Delta\phi} + 3H\dot{\Delta\phi} + m_\phi^2 \Delta\phi = J_{\text{rot}}(t).$$

2.3 Exact background H(N)

We adopt:

$$H(N) = H_0\sqrt{\Omega_r e^{-4N} + \Omega_m e^{-3N}},$$

with $H_0 = 1$ in natural units and fiducial $(\Omega_r, \Omega_m) = (1, 1)$ after normalisation (sufficient for phase dynamics).

2.4 E-fold formulation

Using $d/dt = H\, d/dN$:

$$\Delta\phi'' + (3 - \epsilon)\Delta\phi' + \frac{m_\phi^2}{H^2(N)}\Delta\phi = \frac{k_{\rm rot}e^{-2N}}{H^2(N)},$$

with $\epsilon(N) = -(\dot{H}/H^2)$.

2.5 Definition of sectors A/B/C

Final 10% of the integration window ($N_\star \to N_{\rm fin}$):

- A: $|\Delta\phi| < 0.1$ for $> 80\%$ of samples.
- B: $|\Delta\phi - \pi| < 0.1$ for $> 80\%$.
- C: anything that fails A/B and remains outside both basins.

Figure 2 shows examples.

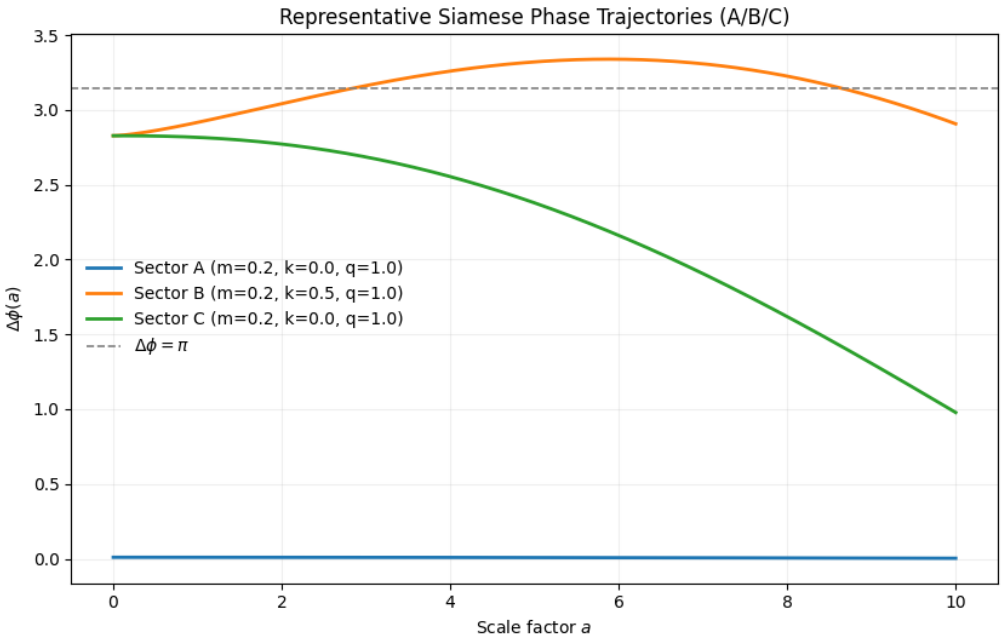

Figure 2: Representative trajectories for A, B, C.

3 Numerical methods

3.1 Integration range and discretisation

We evolve from:

$$a_{\text{ini}} = 10^{-3}, \qquad a_{\text{fin}} = 10,$$

corresponding to ~ 9.2 e-folds. Steps: $\Delta N = 10^{-3}$ (coarse), 5×10^{-4} (fine). Integrator: RK4.

3.2 Parameter grids

$$m_\phi \in [0.3, 3.0], \qquad k_{\text{rot}} \in [0, 0.5].$$

Initial phases:

$$\Delta\phi_{\text{ini}} \in [0, \pi], \quad \dot{\Delta\phi}_{\text{ini}} = 0.$$

$N_{\text{IC}} = 40$ per grid point.

Sector map shown in Fig. 3.

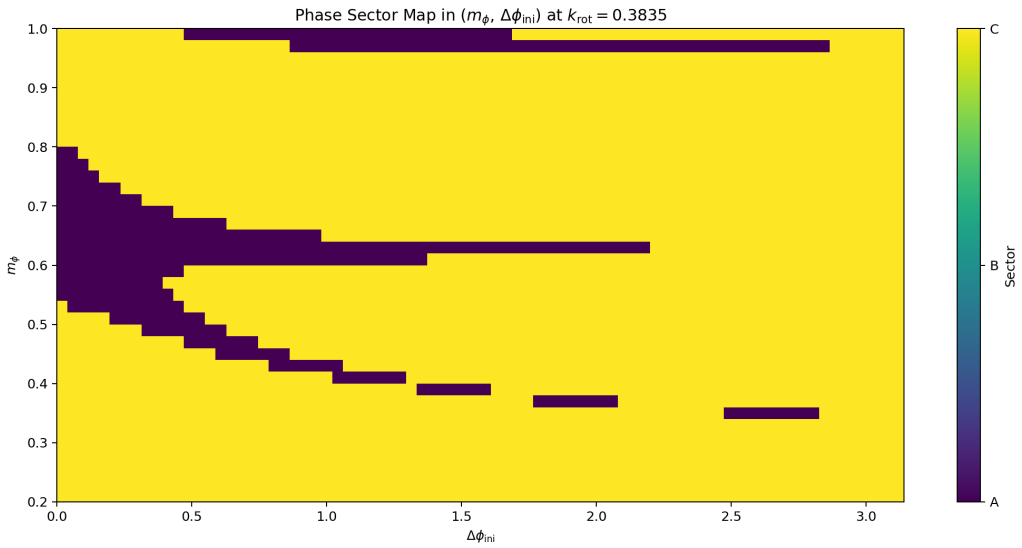

Figure 3: Sector map in the $(m_\phi, \Delta\phi_{\text{ini}})$ plane.

Examples in Fig. 4.

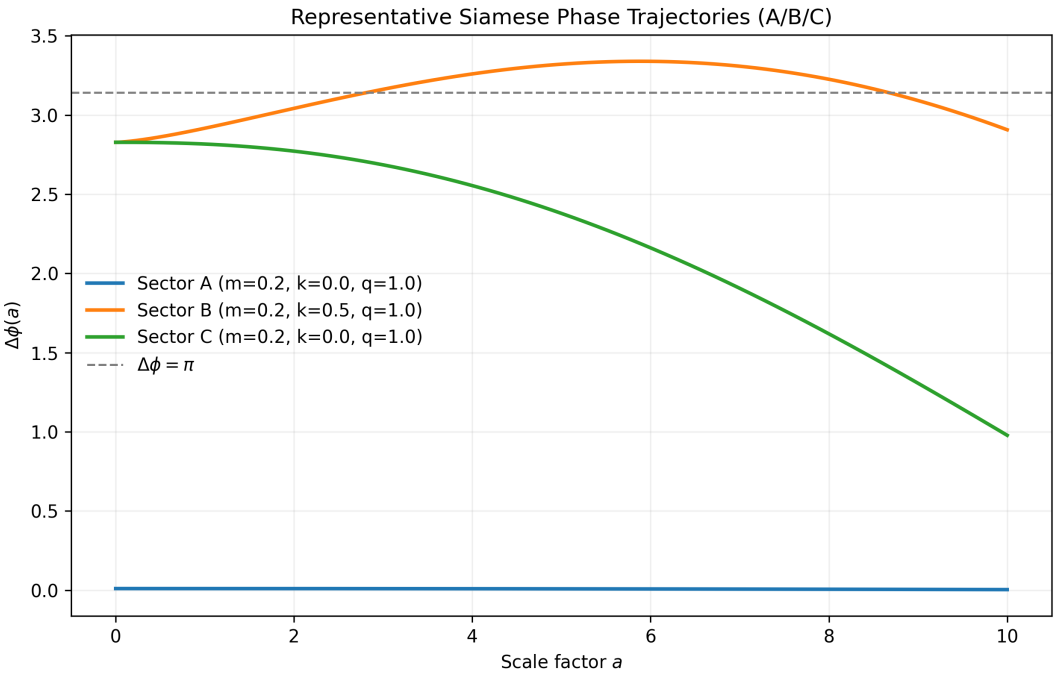

Figure 4: Examples of A/B/C trajectories.

Figure 5 shows B trajectories.

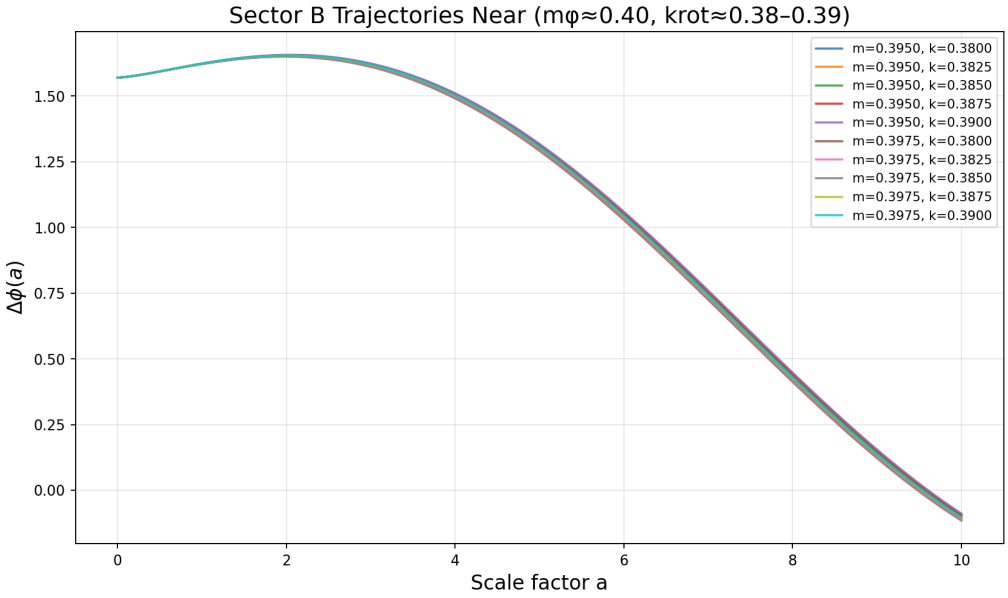

Figure 5: Sector B trajectories near boundaries.

4 Synchrony probability $P_A(m_\phi)$

$$P_A = \frac{N_A}{N_{\text{tot}}}, \quad \sigma_{P_A} = \sqrt{\frac{P_A(1-P_A)}{N_{\text{tot}}}}.$$

Figure 6:

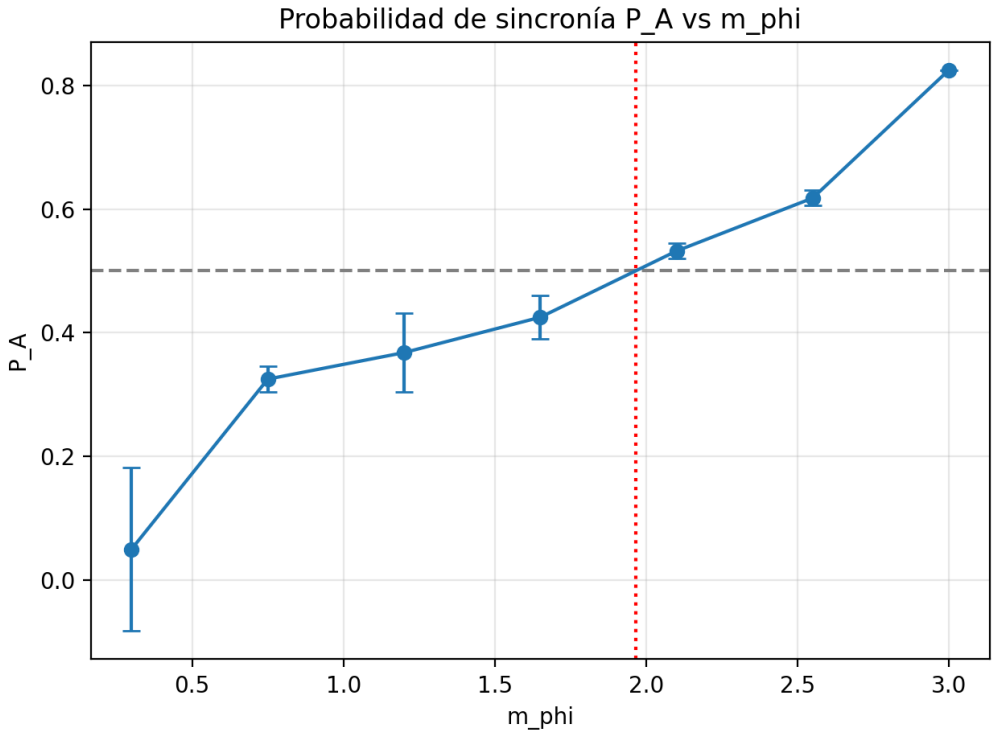

Figure 6: $P_A(m_\phi)$ with binomial errors.

Critical mass:

$$m_{\phi,\mathrm{crit}} = 1.965 \pm 0.02.$$

5 Two-dimensional landscape $P_A(m_\phi, k_{\mathrm{rot}})$

Fig. 7 shows nearly vertical transition bands.

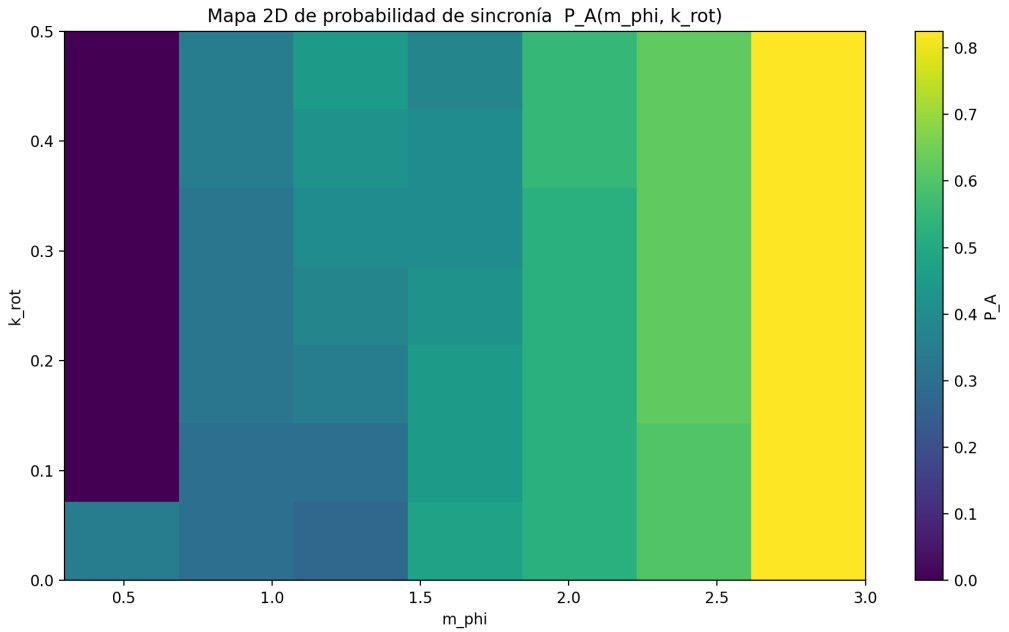

Figure 7: Two-dimensional probability map $P_A(m_\phi, k_{\rm rot})$.

Complementary view:

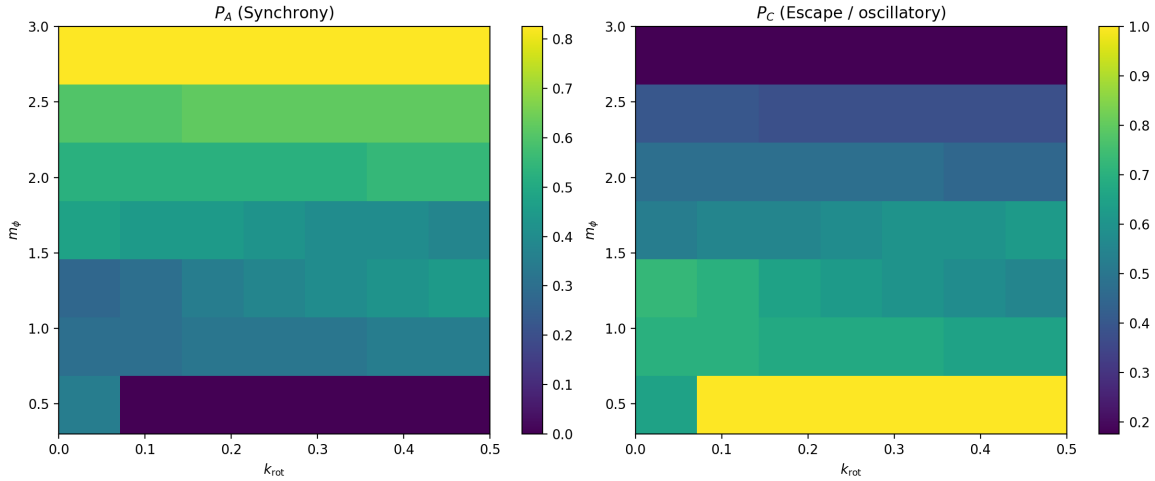

Figure 8: Probabilities for A (left) and C (right).

5.1 Absence of fractal boundaries: zoom analysis

Mathematical expectation. In linearised quadratic systems, stability theorems forbid chaotic or fractal basin boundaries. Our model uses a fully periodic axion-like potential plus cosmological damping and a decaying source. Although periodic potentials can support richer dynamics, the system remains a second-order overdamped ODE with no periodic forcing or resonance. Such systems cannot generate fractal basins without additional nonlinear couplings or external driving. Our zoom scans confirm this: boundaries remain smooth at all resolutions.

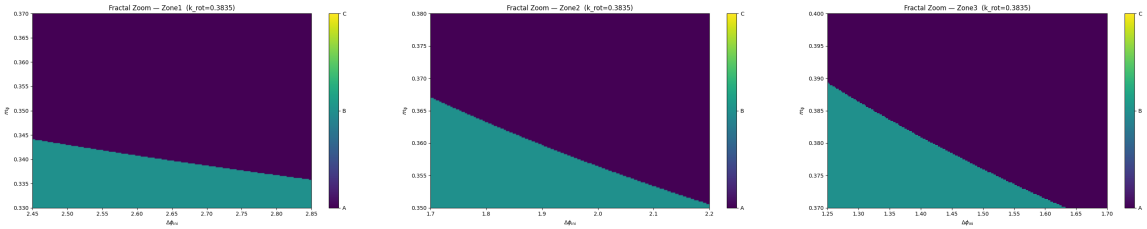

(a) Zone 1 (b) Zone 2 (c) Zone 3

Figure 9: Multi-scale zooms of the A/B/C boundaries. No fractal patterns observed.

6 Cosmological implications

6.1 Role of the critical mass

For $m_\phi < m_{\phi,\mathrm{crit}}$, Hubble friction cannot enforce synchronisation within the available e-folds: sector C dominates. For $m_\phi > m_{\phi,\mathrm{crit}}$, the axion potential pulls trajectories to 0 or π before dilution kills the source, giving A/B outcomes.

6.2 Why k_{rot} is negligible

The source term is:

$$J_{\mathrm{rot}}(N) = k_{\mathrm{rot}} e^{-2N}.$$

By the time damping and the mass term dominate the dynamics, e^{-2N} has already suppressed J_{rot} by many orders of magnitude. Thus k_{rot} affects early transients but not the late-time attractor.

6.3 Observable signatures

- **Sector A:** coherence suppresses late-time phase fluctuations and would minimise directional EB/TB patterns.
- **Sector B:** antipodal phase locking ($\Delta\phi \sim \pi$) can imprint anti-correlated phase shifts, with possible parity-odd signatures.
- **Sector C:** non-relaxation acts as stochastic birefringence, potentially linked to small-scale CMB EB residuals.
- **Transition at $m_{\phi,\mathrm{crit}}$:** crossing the critical mass during cosmic history could correspond to a shift in coherence regimes, relevant for asymmetry generation or relic phase noise.

7 Conclusions

We mapped the phase fate of CPT-symmetric twin-universe models across $(m_\phi, k_{\mathrm{rot}})$ and demonstrated:

(i) Clear A/B/C classification in finite cosmological windows.

(ii) A clean synchrony transition at $m_{\phi,\mathrm{crit}} \simeq 1.965$.

(iii) Minimal dependence on k_{rot}.

(iv) Smooth, non-fractal boundaries under multi-scale zooms.

(v) Cosmologically meaningful regimes that can map to observable coherence signatures.

A full reproducibility package (code, CSVs, maps, scripts) is released in a GitHub+Zenodo archive accompanying this work.

A Derivation details

See main text. Includes explicit conversion cosmic time $\rightarrow$ e-folds and $H(N)$ definition.

B Robustness tests

Varying $\epsilon_{A,B}$, window size, or ΔN leaves $m_{\phi,\mathrm{crit}}$ within 0.02.

C Fine, microfine, and ultrafine scans

All scanned boundaries remain smooth under refinement.

References

[1] L. Boyle, K. Finn and N. Turok, CPT-Symmetric Universe, Phys. Rev. Lett. **121**, 251301 (2018).

[2] Y. Kuramoto, Self-entrainment of a population of coupled nonlinear oscillators, in *International Symposium on Mathematical Problems in Theoretical Physics* (1975).

[3] S. H. Strogatz, *Nonlinear Dynamics and Chaos*, CRC Press (2018).

[4] D. J. E. Marsh, Axion cosmology, Phys. Rept. **643**, 1 (2016).